Effect of Acoustic Resonance on the Dynamic Lift in Square Tube Arrays

Ronald Hanson
McMaster University, Dept. of Mechanical Engineering, Hamilton, Canada
Samir Ziada
McMaster University, Dept. of Mechanical Engineering, Hamilton, Canada

ABSTRACT

The effect of acoustic resonance on the dynamic lift force acting on the central tube in square tube arrays is investigated experimentally for two arrays with spacing ratios of P/D = 2.18 and 3.37. The resonant sound field in the tube array is shown to cause two main effects. First, it produces dynamic lift force on the tube due to the associated acoustic pressure gradient on the surface of the tube, and secondly, it synchronizes vorticity shedding from the tubes and thereby, enhances the aerodynamic lift force due to vortex shedding. The combined effect of these two unsteady lift forces depends on the phase shift between them, which is dictated by the frequency ratio between the frequency of the acoustic mode and that of natural vortex shedding. Therefore, increasing the reduced velocity within the coincidence lock-in resonance range results in rapid variations in the phase shift and consequently in the total lift force. Simple summation of the aerodynamic and acoustic lift forces provides a conservative estimate of the total dynamic lift measured during acoustic resonance.

1. INTRODUCTION

The mechanisms of vortex shedding and acoustic resonance of tube arrays in cross-flow have received considerable attention in the literature because of their importance to industrial applications (see for example, the recent review by Ziada, 2006). Although several authors have reported measurements of the dynamic lift coefficients for tube arrays (e.g. Oengören and Ziada, 1992), the effect of acoustic resonance on these lift coefficients is yet to be determined, and is the focus of the present investigation.

Mohany and Ziada (2006) recently measured the dynamic lift coefficients for a single cylinder in cross-flow during flow-excited acoustic resonance and before the onset of resonance. The results show that the dynamic lift coefficient can increase by a factor of four upon the onset of acoustic resonance. For two tandem cylinders, studied by Mohany and Ziada (2006), similar increases in the lift coefficients were observed. These results suggest that similar trends may occur in tube arrays and emphasize the need for determining the dynamic lift in tube arrays during acoustic resonance.

During acoustic resonance there are two sources of dynamic lift. One source is provided by the sound field. The standing wave excited during resonance causes dynamic lift from the acoustic pressure distribution on the surface of the cylinder. The other source of dynamic lift is provided by periodic vortex shedding from the tubes, which is synchronized and enhanced by the resonant sound field. The present investigation examines the magnitudes and relationships between these dynamic lift components.

2. EXPERIMENTAL SETUP

The wind tunnel is an open loop configuration, consisting of a 50 HP AC induction motor powering a centrifugal type blower which draws air in though the test section. The motor is controlled by a 3-phase, variable frequency inverter allowing fine increment adjustment of flow velocity and repeatability of a selected flow velocity. The test section is a rectangular duct measuring 810 mm in length by 254 mm in height and 76.2 mm in width. The tube spacing and tube diameters are varied to achieve the desired spacing ratios. The inlet of the test section is fitted with a smooth parabolic contraction to reduce pressure drop, prevent flow separation and create a uniform mean flow upstream of the tube array. At the exit of the test section, a diffuser is used to recover the dynamic head. The geometries of the studied arrays are summarized in table 1. The gap flow velocity between the tubes typically ranged from 10 m/s to 80 m/s, corresponding to a Reynolds number range from 10000 to 80000.

Array	*P*(mm)	*D*(mm)	# Row	# Col
P/D = 3.37	50.8	15.08	7	7
P/D = 2.18	36.34	16.67	7	9

Table 1: Dimensions of tested Arrays.

A schematic of a tube array is shown in figure 1. The top and bottom walls are positioned at the

centerline of the flow lanes. A G.R.A.S. 1/4" condenser microphone, mounted flush on the top wall, measures the fluctuating sound pressure directly above the instrumented cylinder. To externally excite the acoustic mode in the absence of air flow, eight loudspeakers are used, four on the top wall and four on the bottom one, as shown in figure 1. While flow-excited acoustic resonance is being investigated, the top and bottom plates and speakers are replaced with solid plates. At the tube instrumented with force transducers, an insert is used on the test section side walls to minimize the gap between the tube and the test section side wall. This gap is maintained at 0.4 mm, which ensured that the cylinder does not contact the walls of the test section. Seals cut from latex are used to prevent flow though the gap. The dynamic lift measurement rig is mounted to a heavy steel frame which is isolated from the ground with vibration pads.

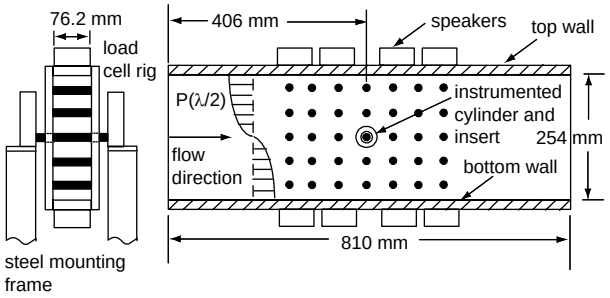

Figure 1: *General tube bundle layout showing the instrumented cylinder.*

The fluctuating lift forces are measured using a rig similar to that constructed by Mohany and Ziada (2006), except that the load cell rig is made stiffer to increase the resonance frequency of the force transducer system beyond the frequency range of turbulence excitation which exists in tube bundles (Paidoussis, 1983). Thus, the lowest natural vibration frequency of the dynamic force transducer is increased to 1800 Hz and the damping ratio is measured to be $\zeta = 0.0013$. This small damping ratio ensured that the phase lag is essentially zero for driving frequencies which are sufficiently lower than the natural system frequency, and therefore no corrective measures are made to phase measurements. The force amplitude, however, is corrected by a magnification factor of 1.16 which is calculated at the acoustic resonance frequency of 680Hz, Rao (2004).

3. ACOUSTIC LIFT FORCE

As illustrated in figure 1, the acoustic mode excited during the experiments consists of a half wavelength standing sound wave between the top and bottom walls of the test section. This standing wave produces time dependant pressure gradients inside the confined test section, with the maximum acoustic pressure at the walls and zero pressure at the middle. This pressure gradient induces surface pressure on the cylinders of the tube array and therefore causes a net periodic lift force on each cylinder. This section investigates the acoustic pressure gradients on the cylinder surfaces, its origins and the magnitude of the induced lift forces.

3.1 Lift force due to sine wave distribution

At the center of the empty test section the vertical pressure distribution of the first transverse acoustic mode yields a sinusoidal pressure distribution with a pressure node at the middle. Assuming this distribution to be valid with tubes present, it is then possible to calculate the amplitude of the dynamic load that would be applied at the tube surface due to an imposed sinusoidal pressure distribution. Feenstra et al (2005) did precisely this and explain the method and mathematical derivation. They proposed an additional component due to the drag force which is induced by the acoustic particle velocity. Feenstra et al (2005) concluded that this drag component is very small and can be neglected. This supposition is found to be true also in the present experiments because the dynamic lift amplitude increased linearly with the acoustic pressure. The dynamic lift amplitude determined from the method suggested by Feenstra et al (2005) is shown in figure 2 as a function of the acoustic pressure on the top wall. It is referred to hereafter as the sine wave distribution lift force.

3.2 Numerical prediction of lift force

For each tube array, the first transverse acoustic mode is simulated numerically. The simulation domain, which corresponds to the actual array geometry, is considered two-dimensional and is meshed with a minimum of 30000 nodes. The surface of the cylinders contains a minimum of 100 equally spaced nodes. The maximum acoustic lift force is induced on the centrally located tube because it experiences the highest pressure gradient. Integrating the acoustic pressure distribution on the surface of this tube for the intermediate and large spacing square tube arrays yields a maximum lift amplitude of 0.0046 and 0.0041 N/m, respectively. These values are normalized to an acoustic pressure of 1 Pa at the top wall of the test section.

Figure 2 shows that the lift force determined from the sine wave distribution (solid line) underestimates the force determined by numerical simulation (dashed line). This difference is due to the distortion caused by the tubes to the sine wave distribution of acoustic pressure. In a related paper, Mohany and Ziada (2007) observed that the acoustic particle velocity distribution was distorted

near the tubes because the acoustic streamlines had to travel around the tubes.

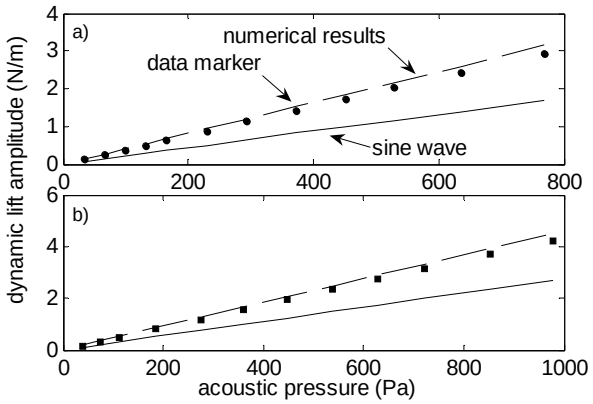

Figure 2: *Acoustic lift force on the central cylinder in square tube arrays obtained experimentally using acoustic excitation only (data points); by means of the numerical simulations (dashed lines); and from the sine wave distribution (solid lines). (a), large spacing; (b), intermediate spacing.*

3.3 Measurements of acoustic lift force

Measurements of the amplitude of the acoustic lift force on the central tube are performed in the absence of flow. Loudspeakers are used to excite the first transverse acoustic mode at various sound pressure levels ranging from 50 to 1000 Pa. The acoustic mode frequency varied slightly from one array to another due to differences in solidity ratio, which is known to influence the effective speed of sound in tube arrays (Parker, 1978).

The experimental data identified by data markers are shown in figure 2. In all the cases, it is found that the measured acoustic lift amplitudes are about 5% lower than the numerically predicted amplitude. This small difference is likely due to the effect of the sidewalls at the tube ends, which is not considered in the two-dimensional numerical simulations. The amplitude of the measured acoustic lift force is seen to increase linearly with the acoustic pressure, which validates this linear relationship assumed in the numerical simulations. These results not only validate the force measuring transducer, but also show that the acoustic sine wave distribution considerably underestimates the acoustic lift force.

4. FLOW-EXCITED RESONANCE

For square tube arrays, there are two mechanisms of acoustic resonance leading to either a pre-coincidence or a post-coincidence resonance. Large spacing in-line arrays exhibit the post-coincidence type resonance, but the intermediate and small spacing arrays exhibit a pre-coincidence acoustic resonance (Ziada and Oengören, 1992, Oengören and Ziada, 1992b).

As illustrated schematically in figure 3, the pre-coincidence acoustic resonance occurs at flow velocities lower than the coincidence flow velocity at which the vortex shedding frequency coincides with the acoustic mode frequency (f_a). In this case, the linear increase in the vortex shedding frequency (f_v) with flow velocity is interrupted by a step up to f_a wherein lock-in occurs between f_v and f_a. Post-coincidence acoustic resonance occurs near the coincidence flow velocity as demonstrated in figure 3. In this case, the resonance frequency can be higher than the vortex shedding frequency ($f_a/f_v>1$) at the onset of resonance. However, as the resonance progresses into the lock-in range, this frequency ratio reverses and the natural vortex shedding frequency becomes higher than the resonance frequency ($f_a/f_v<1$). In the following, two examples are reported: the first is a large spacing array exhibiting a post-coincidence-type resonance, whereas the second is an intermediate spacing array displaying a pre-coincidence-type resonance.

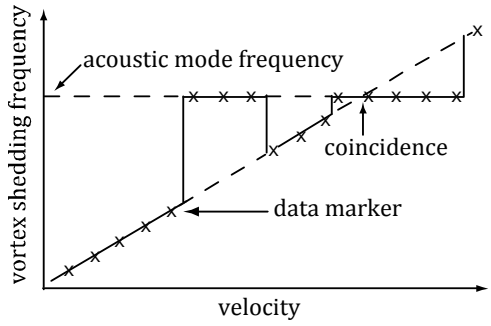

Figure 3: *Schematic of the pre-coincidence and coincidence type acoustic resonances observed in tube bundles.*

4.1 Post-coincidence acoustic resonance: Large spacing array

The aeroacoustic response for the large spacing square array (P/D = 3.37) is presented in figure 4(a). The Strouhal number based on the gap velocity (St_g) is found to be 0.16 and is typical of square arrays with similar spacing ratios (Ziada, 2006; Weaver, 1987). Similarity between this response and that of a single cylinder is evident (Mohany and Ziada, 2005) wherein a post-coincidence-type acoustic resonance is observed. Furthermore, the present results agree well with those reported by Ziada and Oengören (1993) for a large spacing in-line tube bundle, indicating that it is indeed a classical Strouhal excited acoustic resonance. During the lock-in range, the acoustic pressure increases to nearly 3600 Pa_{rms} at a gap velocity greater than the coincidence flow velocity.

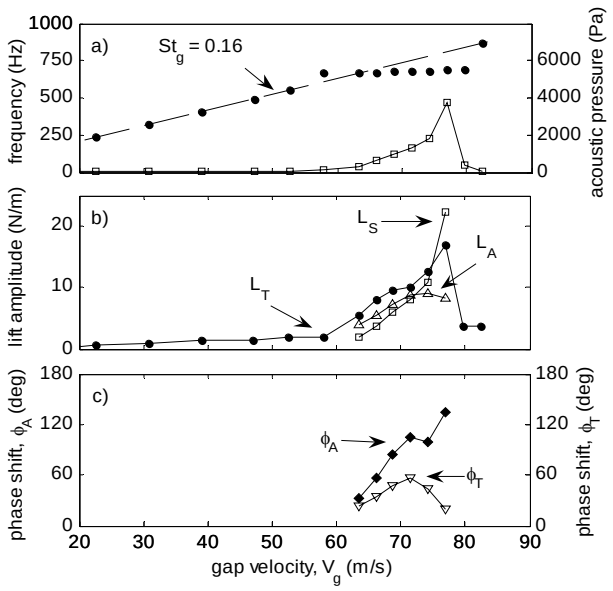

Figure 4. *Aeroacoustic response for the array with P/D=3.37. (a)* •*, frequency of vortex shedding;* □*, amplitude of acoustic mode response; (b)* •*, amplitude of total dynamic lift;* □*, acoustic component of dynamic lift;* Δ*, aerodynamic component of dynamic lift; (c) phase of the total* (∇) *and aerodynamic* (♦) *lift forces with respect to the sound field.*

As the acoustic resonance is initiated, indicated by the sharp increase in the acoustic pressure in figure 4(a), the total dynamic lift amplitude on the centrally located tube, L_T, exhibits a sharp increase as well, figure 4(b). Vortex shedding becomes highly correlated at the resonant frequency, resulting in a decrease in the width of its spectral peak, which is a typical effect of lock-in as discussed by Blevins (1985). Note that the total lift force, L_T, represents the vortex shedding forces alone until the onset of resonance and then it represents the combined effect of acoustic and vortex shedding loading during the lock-in range. The dynamic (acoustic) lift generated by the resonant sound field, L_S in figure 4(b), is calculated from the acoustic pressures measured during flow-excited acoustic resonance. Thus, for each sound pressure measured during the lock-in range, such as those shown by the square data points in figure 4(a), the acoustic lift generated by this sound pressure, L_S, is calculated from figure 2(a), and is plotted in figure 4(b).

When the resonance is initiated, figure 4(b) shows that the total dynamic lift amplitude, L_T, is greater than the predicted lift caused by the sound field alone, L_S. However, the difference between these lift components decreases with flow velocity until the acoustic component L_S actually exceeds the total lift amplitude near $V_g \approx 75$m/s. The reason for this can be deduced from the measured phase shift, ϕ_T, between the sound pressure acting on the top of the test section and the total dynamic lift measured by the load cells.

Figure 5 shows two vector diagrams depicting the dynamic lift amplitudes with their phases relative to the sound pressure on the top wall. The two diagrams correspond to gap velocities of 66 and 76 m/s and are plotted with different scales for the sake of clarity. In the absence of flow, the phase difference between the dynamic lift L_S and the sound pressure on the top wall is zero. Since L_T, L_S and ϕ_T are known from the measurements, the vector diagrams can be constructed for various flow velocities within the lock-in range. In addition, the total lift can be decomposed into its two components; namely the acoustic lift, L_S, and the aerodynamic lift, L_A, which is generated by vortex shedding excitation. The phase angle, ϕ_A, between the aerodynamic, or vortex shedding, lift and the excited sound field can also be found from these vector diagrams. Figures 4(b) and (c) show the resulting values of the aerodynamic lift, L_A and its phase ϕ_A.

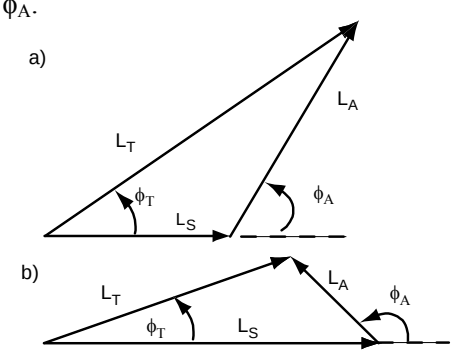

Figure 5. *Vector representation of the dynamic lift forces during acoustic resonance for the square tube array with P/D=3.37.* (a) $V_g = 66$ *m/s; (b)* $V_g = 76$ *m/s.*

Figure 4(b) shows the three lift force components during acoustic resonance. At the beginning of acoustic resonance range, L_T, is greater than either of the aerodynamic or sound components. The vector diagram of this case is shown in figure 5(a). Since the phase angle ϕ_A between L_A and L_S is small, the total lift is larger than either of them. As the flow velocity is increased, ϕ_A increases because of the resulting decrease in the ratio f_a/f_v. At $V_g \approx 76$ m/s, the phase angle ϕ_A increases to 135°, as shown in figure 5(b), and the total dynamic lift force becomes smaller than the dynamic lift force predicted from the sound field alone.

4.2 Phase comparison with the literature

Mohany and Ziada (2007b, 2006) performed similar tests on single and tandem cylinders,

respectively. They also used the method of Feenstra et al (2005) to estimate the value of L_S, and found it to be very small, on the order of a few percent of the measured L_T during resonance. Therefore, the phase measured between the microphone at the top wall and the dynamic lift on the cylinder is essentially the phase shift between the sound field and the aerodynamic lift on the cylinder. The present phase results for the large array are compared with those of Mohany and Ziada (2007b) in figure 6. The abscissa in this figure is the ratio of the acoustic resonance frequency to the natural vortex shedding frequency, f_a/f_v. The latter is based on the natural Strouhal number observed away form resonance effects, which is determined to be 0.16 from figure 4(a). As can be seen in figure 6, there is a relatively good agreement between the trend of present results and that reported for a single cylinder by Mohany and Ziada (2007b). This agreement substantiates, beyond doubt, the measured intrinsic phase relationships between the resonant sound field, the vortex shedding lift force and the total lift force on the tube.

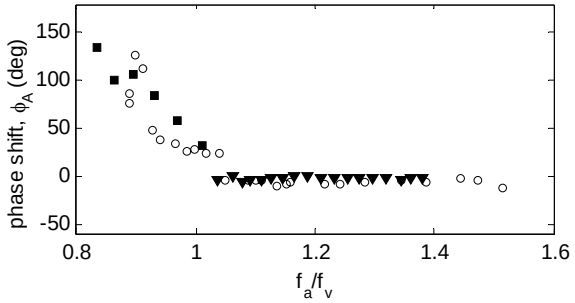

Figure 6. *Phase shift, ϕ_A, between the aerodynamic lift force and the acoustic pressure field.* ■, *P/D=3.37;* ▼, *P/D=2.18;* ○, *single cylinder from Mohany and Ziada (2007b).*

4.3 Pre-coincidence acoustic resonance: Intermediate spacing array

The aeroacoustic response for the square tube array with P/D = 2.18 is shown by figure 7(a). The maximum acoustic pressure amplitude reaches approximately 8000 Pa_{rms}, or 172 dB. A characteristic of this array is the slight modulation in the acoustic pressure amplitude with the flow velocity within the lock-in region. As the flow velocity is increased, after the onset of acoustic resonance, the acoustic pressure increases continuously until the maximum flow velocity of the test section.

A single Strouhal number of 0.164 is identified before the onset of acoustic resonance and is consistent with published data (Ziada, 2006). Acoustic resonance occurs before coincidence of the natural vortex shedding with the acoustic mode frequency. This is a typical example of a pre-coincidence acoustic resonance. Similar response has been observed in the literature for intermediate and small spacing in-line tube arrays, see for example Ziada and Oengören (1990, 1992). For these spacing ratios, Oengören and Ziada (1992b) demonstrate that the flow instability causing acoustic resonances is basically different from the symmetrical jet instability that causes constant Strouhal number vorticity shedding in the absence of acoustic resonance. Acoustic resonance occurs due to coupling between the resonant mode and the unstable shear layers formed between the tubes.

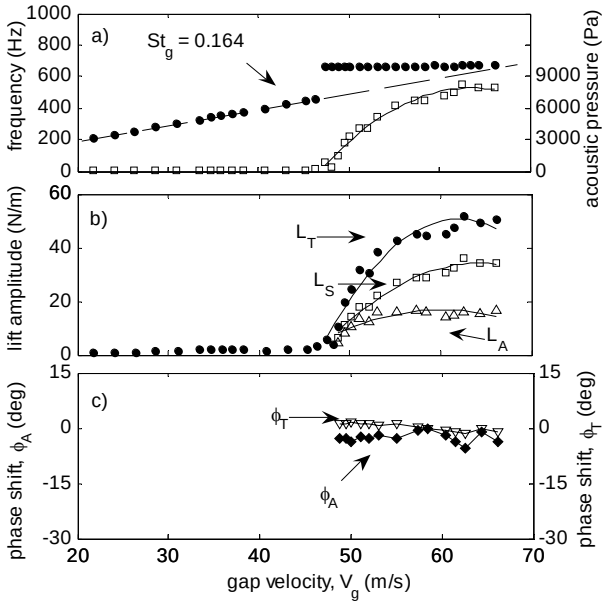

Figure 7. Aeroacoustic response for the array with P/D=2.18. (a) •, frequency of vortex shedding; □, amplitude of acoustic mode response; (b) •, amplitude of total dynamic lift; □, acoustic component of dynamic lift; Δ, aerodynamic component of dynamic lift; (c) phase of the total (∇) and aerodynamic (♦) lift forces with respect to the sound field.

Much like the change in the acoustic pressure, the dynamic lift experiences a large increase in amplitude during acoustic resonance, as shown in figure 7(b). The measured acoustic pressures within the lock-in region shown in figure 7(a) are used to calculate the dynamic lift values due to sound alone, L_S, and are given in figure 7(b). It is seen that the total dynamic lift, L_T, is always higher than the acoustic lift force, L_S. Furthermore, the phase shift, ϕ_T, between the total lift, L_T, and the acoustic field dynamic lift, L_S, is essentially zero throughout the resonance range. The calculated aerodynamic lift component, L_A, which is shown in figure 7(b), can be linearly summed with the acoustic dynamic lift, L_S, with little error to estimate the total dynamic lift

in this case. This is because the calculated phase shift, ϕ_A, between the aerodynamic lift, L_A, and the acoustic dynamic lift, L_S, is essentially zero throughout the resonance range. The calculated phase shift, ϕ_A, is overlaid on the data of Mohany and Ziada (2007b) in figure 6, and is seen to agree well with the flat phase response over the relevant range of frequency ratios, which corresponds to the pre-coincidence resonance.

5. CONCLUSIONS

The effect of acoustic resonance on the dynamic lift forces acting on the tubes of square tube arrays is investigated experimentally. Numerical predictions of the acoustic lift force agree well with the experimental results. The sine wave distribution underestimates this lift force because it does not account for the distortion of the acoustic mode by the presence of the tubes.

The pre and post-coincidence acoustic resonances exhibit distinct dynamic lift characteristics.

For the post-coincidence resonance, the dynamic lift characteristics are complex and depend on the phase between the resonant sound field and the aerodynamic lift generated by vortex shedding. This phase is shown to change rapidly within the lock-in region. The total dynamic lift therefore may be larger or smaller than the acoustic dynamic lift. A conservative estimate of the total dynamic lift may be obtained by summing the acoustic and the aerodynamic lift forces.

Throughout the pre-coincidence resonance, the aerodynamic lift is nearly in phase with the resonant sound field and the resulting acoustic dynamic lift. A simple linear summation of the dynamic lift due to sound with the aerodynamic lift due to vortex shedding predicts the total dynamic lift well.

6. REFERENCES

Blevins, R., Bressler, M., 1993, Experiments on acoustic resonance in heat exchanger tube bundles. *Journal of Sound and Vibration*, **164**, 502-534.

Feenstra, P. et al, 2005, Acoustic resonance in a staggered tube array. *Journal of Fluids and Structure* **21**: 89-101.

Mohany, A., Ziada, S., 2005, Flow-excited acoustic resonance of two tandem cylinders in cross-flow. *Journal of Fluids and Structures* **21**: 103-119.

Mohany, A., Ziada, S., 2006, Effect of acoustic resonance on the dynamic lift forces acting on two tandem cylinders in cross-flow. *ASME PVP Conference*, Vancouver.

Mohany, A., Ziada, S., 2007a, Effect of cylinder diameter on the resonance mechanism of two tandem cylinders in cross-flow. *Journal of Pressure Vessel Technology* (in press).

Mohany, A., Ziada, S., 2007b, Effect of flow-sound interaction on the dynamic lift force of a single cylinder in cross-flow. *Dynamics of Continuous, Discrete and Impulsive Systems*, Series A (in press).

Oengören, A., Ziada, S., 1992, Unsteady fluid forces acting on a square tube bundle in air cross-flow. *ASME HTD*, **230**: 55-74.

Oengören, A., Ziada, S., 1992b, Vorticity shedding and acoustic resonance in an inline tube bundle part II: Acoustic resonance. *Journal of Fluids and Structures*, **6**: 293-293.

Paidoussis, M., 1983, A review of flow-induced vibrations in reactors and reactor components. *Nuclear Engineering Design*, **74**: 31-60.

Parker, R., 1978, Acoustic resonances in passages containing banks of heat exchanger tubes. *Journal of Sound and Vibration*, **57**: 245 – 60.

Weaver, D. S. et al, 1987, Strouhal numbers for heat exchanger tube arrays in cross flow. *Journal of Pressure Vessel Technology,* **109**: 219-223.

Ziada, S., Oengören, A., 1990, Flow-induced acoustical resonance of in-line tube bundles. *Sulzer Technical Review*, **1**: 45 47.

Ziada, S., Oengören, A., 1992, Vorticity shedding and acoustic resonance in an in-line tube bundle part I: Vorticity shedding. *Journal of Fluids and Structures*, **6**: 271-292.

Ziada, S., Oengören, A., 1993, Vortex shedding in an in-line tube bundle with large tube spacings. J*ournal of Fluids and Structures*, **7**: 661 – 687.

Ziada, S., 2006, Vorticity shedding and acoustic resonance in tube bundles. *Journal of the Brazilian Society of Mechanical Sciences and Engineering,* **28** (2): 186 – 199.